Research Article

SOHAG JOURNAL OF SCIENCES

https://doi.org/10.21608/sjsci.2023.185274.1053

Magmatism and Related Mineralizations in Wadi Hammad, North Eastern Desert, Egypt

El Sayed A. Saber*, Mohamed H. Ali, Ahmed A. El-Sheikh

Geology Department, Faculty of Science, Sohag University, Sohag 82524, Egypt.
**E-mail: elsayedahmed@science.sohag.edu.eg, new_sayed@yahoo.com*

Received: 3rd January 2023, **Revised:** 21st January 2023, **Accepted:** 22nd January 2023.
Published online: 1st May 2023

Abstract: Mineralization in the Wadi Hammad area is represented by polymetallic vein-type and occurs in four modes, they are mineralized main quartz vein, silicified shear zone, associated hydrothermal alterations, and breccia zones. They mainly occur in the contact between Dokhanvolcanics and Younger granites and are confined to and controlled by the Wadi Hammad shear zone. The study revealed that Dokhan volcanics have adakitic nature and are formed by slab melt. Accordingly, these rocks are favorable sites for the formation of Au-(Cu)deposits. Hammad granite rocks are characterized bymetaluminous to weakly peraluminous, span the boundary between the ilmenite-magnetite series, transitional between moderately and strongly oxidized granites, situated a relatively shallow to moderate depths (20 to 30 km), and started to crystallize at temperatures around 800 °C. It is suggested that mineralization in WadiHammad formed due to intrusion of the strongly oxidizing, water- and volatile-rich, and alkaline to alkalie-calcic magma into the adakiticDokhan volcanic leads to circulation of these fluids in the latter leaching the available metals (Au and base metals). The leached metals are deposited in preexisting open fissures at the cold end of convective cells near the surface form Au (Cu)-rich quartz veins.
Keywords: Au-(Cu)mineralization, magmatism, volcanism, adakitic nature, hydrothermal.

1. Introduction

The Arabian Nubian shield in the Eastern Desert of Egypt constitutes one of the longest metallogenic belts containing Au-bearing quartz vein and hydrothermal systems in Africa. Most of these mineralizations are related to intensive multiple-aged magmatism events that took place in different tectonic settings due to different tectonic processes such as; subduction, accretion of island arcs, continental collision, lithosphere delamination or slab melt. The close of the Pan-African was characterized by a change from subduction and arc-related magmatism to post-tectonic alkaline magmatism **[1].** Porphyry-Cu and epithermal deposits are genetically associated with arc magmas displaying a broad range of compositions, from low-K calc-alkaline, through high-K calc-alkaline, to alkaline (e.g., **[2-4]**. In the North Eastern Desert of Egypt, granitoids and their related mineral deposits (particularly Sn-W-Ta-Mo-U-REE mineralization **[5]**, porphyry Cu-Mo-Au (Um Monqul porphyry located to the north of the study area) **[6]** and hydrothermal vein-type gold **[7]**, are showing coeval association. On the other hand, a special association between adakites and of large number of porphyry and epithermal deposits has been provided by many authors **[8-10]**. In the North Eastern Desert of Egypt adakitic lavas were recorded in wide area **[11]**. In Wadi Hammad gold mineralization is one of the few mineralizations related to the emplacement of the calc-alkaline and alkaline granites at (610–590 Ma), and the contemporaneous eruption of the late-orogenic Dokhan volcanic. These mineralizations are located in the boundary between younger granite and Dokhan volcanic rocks. However, plate tectonic, volcanism and magmatism are the main geological factors controlling ore mineralization **[12-17]**. Hammad Au-(Cu) mineralization has been the subject of several geological studies **[18-21]**, but there is limited knowledge of the volcano-plutonic association history and its related mineralization. This study aims to understand the geological, petrographical, and geochemical characteristics and the evolution of Dokhan volcanic and intrusive granitic rocks in Wadi Hammad, North Eastern Desert, Egypt. In addition, the present work aims to understand the relationship between magmatism, the adakitic nature of most rocks, and their relation to the metallogenesis of high-grade vein-type deposits in the study area.

2. Geological setting

The present study is concerned with the volcano-plutonic association in the Wadi Hammad area. This area is located at the western boundary of the Arabian-Nubian Sheild and lies between latitudes 26° 58′ and 27° 10′ N and longitudes 32°50′ and 33°02′ E **(Fig. 1A)**. The Hammad area lies in the northern sector of the Eastern Desert, to the west of GabalDokhan type locality and to the south east of Guluf granitic mass. The studied area includes Neoproterozoic granitoids, volcanic rocks, and Hammamat sedimentary units; these rocks are cut by basic tykes **(Fig. 1B)**. Field relation indicated that the volcanic rocks and Hammamat sedimentary rocks are older than the granites **[22]**, where these volcanic and sedimentary rocks intruded by post tectonic younger granite **(Fig. 2A)**, the latter contains, xenoliths and enclaves of volcanic rocks. Dokhan volcanics at Wadi Hammad are the main rock units and were the subject for many research workers **[18-20, 23-26]**.

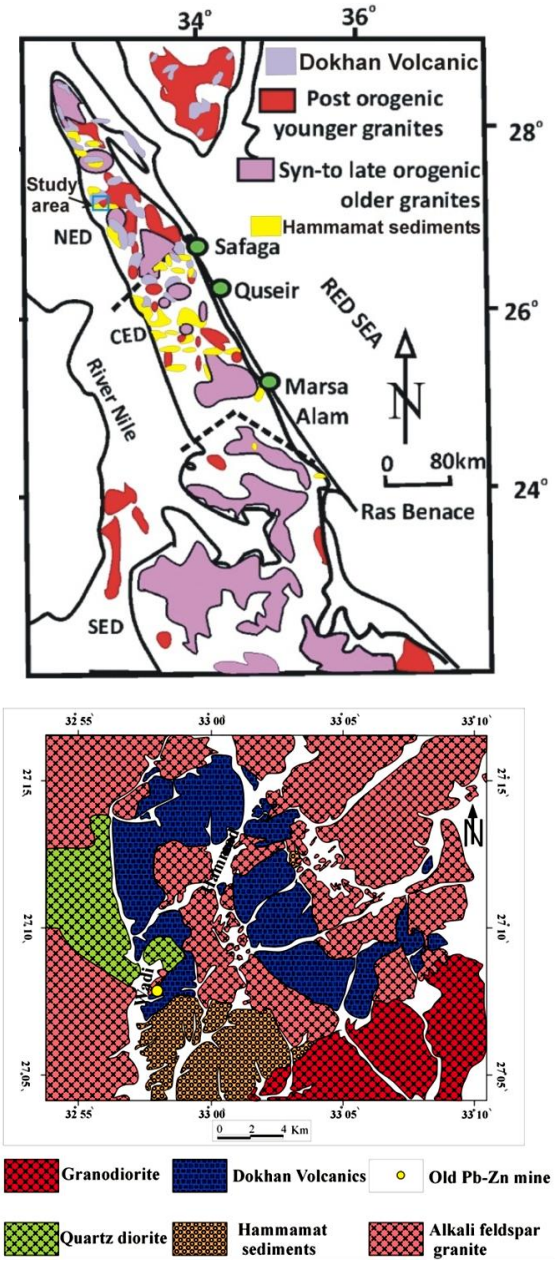

Figure 1. A) Location map of the study area, **B)** Geological map of the study area.

The Dokhan volcanics are represented by moderately to high-relief mountainous ranges in colors from grey, greenish-grey, to reddish-brown. They mainly consisted of andesites, dacites, rhyodacites, and rhyolite porphyry and the associated pyroclastics. Field observation indicates that felsic varieties are more common and are commonly crop out at the north western part of the area and at the Wadi Hammad mine locality. These felsic volcanic rocks are characterized by well stratified appearance and composed of well-banded acidic welded tuffs (Ignimbrite; **Fig. 2B)**, agglomerates alternated with lava flows. The intermediate volcanic rocks crop out mostly along the northeastern and south western parts of the area and consistent the lower part of Dokahn volcanic succession. They are composed of pyroclastics (agglomeratesand lithic tuffs) alternating with porphyritic andesite flows **(Fig. 2C)**. The Hammamat sediments bound the Dokhan volcanic from the south. The contact is intercalations of the two units where the upper part of the Dokhan volcanics is intercalated with greywacke and conglomerate of the overlying Hammamat sediments. The Hammamat sediments are represented by thickly bedded succession, about 8 m thick of siltstones, greywacke, conglomerate **(Fig. 2D, E)**. Younger granites are exposed at the western side of Wadi Hammad area, the granites grade in colour from pinkish white to light pink colour, they are medium to coarse coarse-grained **(Fig. 2F)**, form high rough mountains with rugged peaks. The granite mass intrudes the Dokhan volcanics along the eastern bank of Wadi Hammad and Hammamat sediments (conglomerates) in the western side ofWadi Hammad, the contact between these granites and Dokhan-Hammamat succession is sharp, steep andresulted in tilting of the succession to the east. The granitic rocks are well jointed and dissected by numerous faults and shear zones.

3- Material and methods

During field work the main mineralization site was descried and measured also representative samples from ore deposits and country rocks were collected for petrographic and geochemical studies. More than 25 polished-thin sections were prepared for the microscopic examination by using a transmitted and reflected light Polarizing Microscope. 24 samples of Dokhan volcanics and 10 samples of granite country rocks were geochemically analyzed for both major (in wt%), trace elements (in ppm), and Rare Earth Elements (REEs). The geochemical analysis was done by a Philips x-ray fluorescence technique model PW/2404, with Rh radiation tube. For the major composition, the detection limits are between 0.001 and 0.03%, and 0.5 ppm. for Loss on ignition (L.O.I), while the detection limits for the trace element contents range between 0.01 and 0.5 ppm. REEs contents were analyzed using the inductively coupled plasma-mass spectrophotometry technique (ICP-MS) (720 ICP-OES, Agilent Technologies), with the detection limits of 0.1 ppm. all the geochemical analyses were done at the Central Laboratories of the Geological Survey of Egypt.

3. Results

3.1. Petrography

3.1.1. Dokhan Volcanic

Andesite rocks are generally massive, fine to medium-grained, and of grey, greenish-grey, and pale violet colors. They are composed mainly of euhedral to subhedral plagioclase with fewer amounts of amphibole and clinopyroxene phenocrysts set in a hyalopilitic and pilotaxitic groundmass **(Fig. 3A)**. Accessory minerals are represented by opaques and apatite; and the secondary minerals are sericite, chlorite, and calcite. Plagioclase is predominantly saussuritized, other crystals show zoning. Clinopyroxene phenocrysts represented by microphenocrysts of augite showing corroded edges due to replacement by chlorite, and iron oxides along their grain margins **(Fig. 3B)**. Amphibole displays subhedral to euhedral, prismatic phenocrysts. The groundmass is composed of plagioclase laths, amphibole, augite, biotite and opaque minerals. The groundmass

components show intense alteration to chlorite, epidote, and iron oxides. Dacite is massive, fine-to medium-grained, porphyritic, ranges in color from pale red to pinkish-red. It composed mainly of plagioclase phenocrysts as the main component with fewer amounts of biotite, amphibole and quartz phenocrysts, set in a microcrystalline groundmass of the same composition **(Fig. 3C)**. The accessory minerals are apatite, zircon and iron oxides and secondary minerals represented by epidote, chlorite and sericite. Plagioclase phenocrysts are subhedral to euhedral, their size of about 3.0x1.5 mm, characterized by zoning and are slightly to moderately altered to secondary minerals of sericite and epidote. Biotite and amphibole altered to chlorite and iron oxides. The groundmass is more susceptible to alteration than the phenocrysts. Rhyodacite is well-developed porphyritic texture, light color than dacite rock, it is pink, buff, cream, reddish brown, composed of phenocrysts of plagioclase, K-feldspar and quartz phenocrysts with very less amount of biotite, the phenocrysts embedded in microcrystalline groundmass similar to the phenocrysts in composition **(Fig. 3D)**. Apatite and zircon are the main accessory minerals and the secondary minerals represented by sericite and epidote. The plagioclase and K-feldspar are slight to moderately altered to secondary minerals. The groundmass is characterized by micro granular and locally spherulitic textures. Rhyolite is fine- to medium-grained, red color, porphyritic with an abundance of phenocrysts of K-feldspar and quartz with less amount of plagioclaseand rare microphenocrysts of biotite, they are set in microcrystalline groundmass. The phenocrysts occur either as discrete crystals or cumulated from glomerophyric aggregates **(Fig. 2E)**, the phenocrysts altered mainly to sericite. The accessory minerals are represented by apatite and zircon. Pyroclastic rocks are represented by ignimbrite, agglomerate, and several varieties of tuff. Ignimbrites is welded and unwelded, mainly associated with rhyolite and reflect the rhyolitic composition, composed of fiamme, glass shards, crystals, crystal fragments (of plagioclase, K-feldspar and quartz), and scarce felsic rock fragments, set in glassy groundmass and show well defined foliation **(Fig. 3F)**. Agglomerates composed of rock fragments and crystal fragments, the former represented by rounded to subrounded volcanic rock fragments (up to 3cm in size) mainly of porphyritic andesite and dacite. The crystal fragments are observed in the groundmass as plagioclase, K-feldspars, and quartz. The rock fragments and crystal fragments set in glassy groundmass of tuff, lithic and crystal fragments. Tuff varieties include lapilli and crystal tuffs, lapilli tuffs are composed of angular to subangular crystal fragments mainly of plagioclase, quartz, opaque minerals, rare K-feldspars and mafic minerals. Lithic fragments represented by porphyritic andesite, dacite and rhyolite. All the components are embedded in glassy or tuffaceous groundmass consist of fine plagioclase and quartz fragments.

3.1.2. Granite

The granitic rocks formlow to moderate circular hills, medium-to coarse-grained, holocrystalline, equigranular, and range from pinkish white to light pink color. They are well jointed showing well developed cutting jointing pattern, altered due hematization and secondary silicification. They are composed of quartz and K-feldspars with subordinate amount of plagioclase, in addition to less amount of muscovite and lesser amount of biotite **(Fig. 4A)**. Zircon, apatite, and opaques represent the accessory minerals, while the secondary minerals represented by carbonated sericite, chlorite and epidote. They are characterized by well-developed hypidiomorphice qui-granular texture; porphyritic and poikilitic textures are also common **(Fig. 4B)**. Quartz is the most forms up to 30 % by volume and occurs as interlocked grains up to 4 mm in size, with serriform grain boundaries, quartz locally replaces feldspars, particularly plagioclase ones along their grain boundaries. Alkali feldspars are repsented by othoclase, perthite othoclase, microcline orthoclase. They are euhedral to subhedral simply twinned prismatic crystals range in size from 0.2 to 0.5 mm in length. They are altered to kaolinite and sericite. Plagioclase occurs as subhedral tabular-shaped crystals showing carlsbad and pericline twinnings, display moderate alteration to sericite and clays. Muscovite occurs euhedral laths up to 1.5 mm long and display disposed pattern due to subparallel alignment particularly in the deformed varieties, secondary muscovite distinguished by shreds that replaced plagioclase along their grain bounderies **(Fig. 4C)**.

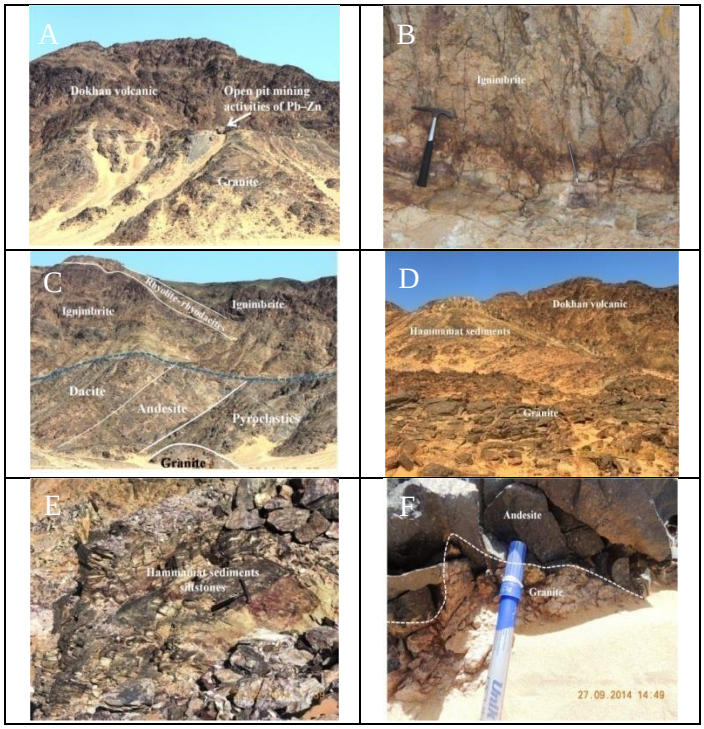

Figure 2: A- Dokhan volcanic rocks intruded by post tectonic younger granite; B- well stratified Ignimbrite on the upper felsic Dokhan volcanic; C- The intermediate volcanic composed of pyroclastics alternating with andesite flows; D- Hammamat sediments and Dokhan volcanic intruded by younger granite; E- Hammamat sediments are represented by thickly bedded succession of siltstones; F- Medium to coarse coarse-grained younger granite intruded in andesite flows.

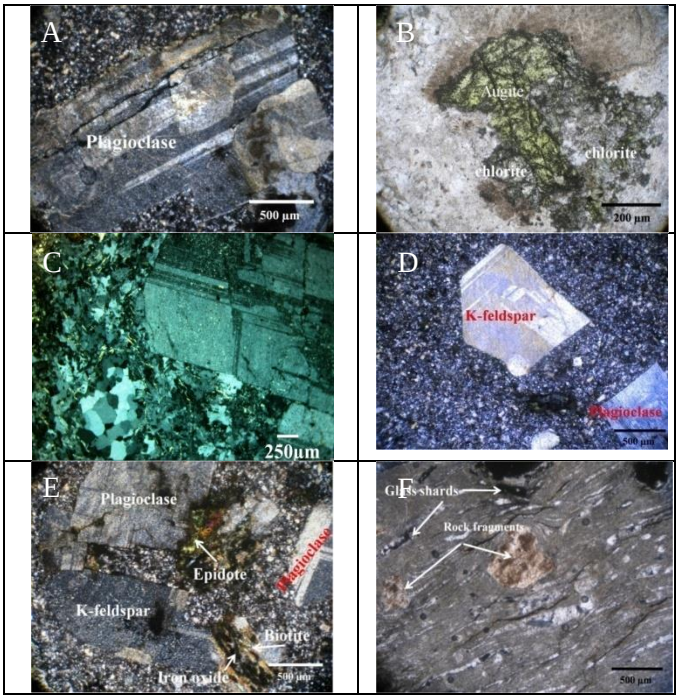

Figure 3: A- andesite rock, euhedral plagioclase phenocrysts set in a pilotaxitic groundmass; B- andesite rock, augitephenocrysts corroded along their grain marginsby chlorite; C- Daciterock, composed mainly of plagioclase phenocrystsset in a microcrystalline groundmass D- Rhyodacite rock, plagioclase and K-feldspar with less amount of biotitephenocrysts, set in a microcrystalline groundmass of the same composition; E- Rhyolite, K-feldspar and plagioclase phenocrysts cumulated from glomerophyric aggregates; F- Ignimbrite, fiamme, glass shards, and scarce felsic rock fragments, set in well defined foliation glassy groundmass.

3.1.3. Mineralization

Mineralization in Wadi Hammad area represented by polymetallic type and occur in four modes; the mineralized main quartz vein, silicified shear zone, the associated hydrothermal alterations and breccia zones, they are mainly confined to and controlled by Wadi Hammad shear zone. Quartz vein occur in the center part of the shear zone of about 1m in width and extends for about 500 meters along the strike of the shear zone. Quartz vein composed of white to smoky quartz characterized by vuggy, colloform and comb structures. The ore minerals represented by massive ore, disseminated sulphides (Arsenopyrite, pyrite, chalcopyrite, galena and sphalerite), vuggy and fracture filling types (mainly sphalerite and galena, **Fig. 4D)**. Silicified shear zone affected the contrary Dokhan volcanic and extending more than 2 meter in width around the main quartz vein. Silicification represented by siliceous-rich materials with red color appearance may be due to highly oxidation of base metal sulfides (jasper like). In additions to quartz veinlets/selvages that are cut the silicified shear zone see Fig **4D** and **E**. The hydrothermal processes resulted in formation of alteration zones around the mineralized quartz vein **(Fig. 4E)** of about 5-meter width. These alteration zones have unique mineral which can be used to distinguish the alteration zones into, sericitic and quartz- chlorite–epidote-pyrite alteration zones. Breccia zone occur on the distal country rock and the sheared quartz vein, their type is varied according to clast lithology, size, shape and cement composition. In the distal country rock breccia zone composed of angular to subangularclasts of host rocks, their size ranges from 1mm to tens of cm. The clasts are embedded matrix of sphalerite and galena **(Fig. 4F)**. In quartz vein, breccia zone composed of fine to medium-grained quartz clasts and fragments of about 0.5 to 3 cm in length and cemented by ferruginous material of iron oxide and/or sulfide minerals of sphalerite and galena.

3.2. Geochemistry

3.2.1. Dokhan volcanic

The studied Dokhan volcanics show a wide range of compositions (SiO_2 ranges from 57.844 to 72.3 wt%, Al_2O_3 ranges from 14.096 to 16.224, Fe_2O_3 ranges from 2.046 to 6.73, CaO ranges from 0.724 to 4.782, Na_2O ranges from 4.56 to 5.34, MgO ranges from 0.358 to 3.314, K_2O ranges from 2.394 to 3.954, TiO_2 ranges from 0.418 to 1.332, MnO ranges from 0.076 to 0.104 and P_2O_5 ranges from 0.058 to 0.372 and LOI ranges from 0.524 to 1.806 (Fig.5A). Trace elements are showing a common enrichment of large ion lithophile elements (LILE), such as Ba, Sr, Zr, Pb and Rb as well as the high field strength elements (HFSE) such as Zr and LREE (Fig.5B). REE have slightly fractionated patterns with an elevated light (LREE) and depleted heavy (HREE) with enrichment in Ce, La and Nd, negative Eu anomaly is characteristics for the more felsic lavas (Fig.5C) which may be suggests fractionation of hornblende with plagioclase from basaltic andesite of the same suite.

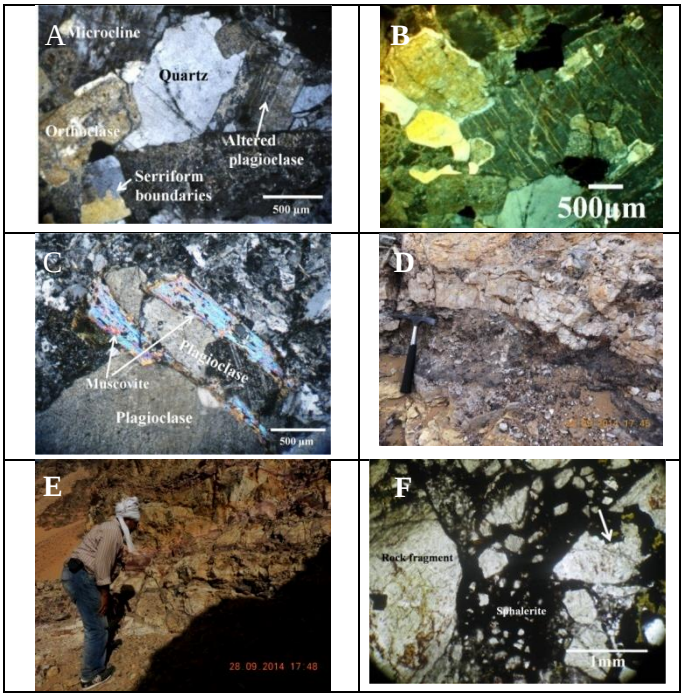

Figure. 4: A- Granitic rocks, composed of quartz and K-feldspars with subordinate amount of plagioclase; B- Granite rock, porphyritic texture; C- Granite rock, muscovite shreds replaced plagioclase along their grain bounderies; D- Mineralized quartz vein, characterized by vuggy, colloform, comb structures, and vuggy, fracture filling ore-types mainly sphalerite and galena; E- Hydrotherma alteration zones around the mineralized quartz vein; F- Breccia zone, composed of angular to subangularclasts of host rocks embedded matrix of sphalerite and galena.

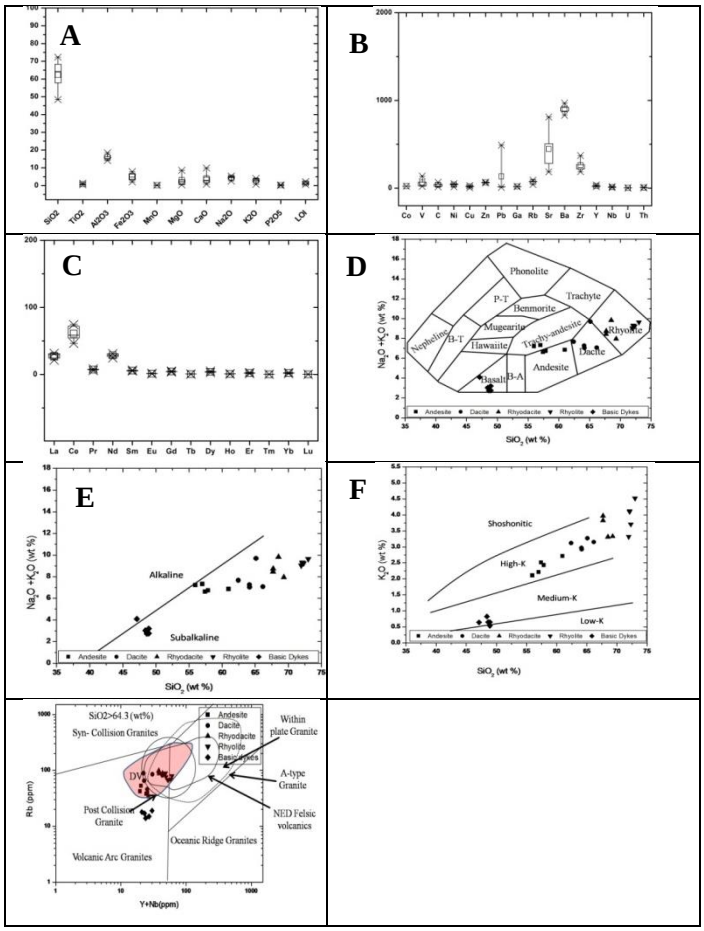

Figure 5: A, B and C- Box plot graphs showing the summary of geochemical data for Dokhanvolcanics of major oxides (wt%) (A), trace elements (ppm) (B) and REE (ppm) (C); D- Total alkali versus silica (TAS) classification using diagram [27] plots of Dokhan volcanic lava flows; E- SiO_2 versus K_2O+ Na_2O plots showsubalkaline characteristics of Dokhan volcanic; F- K_2O–SiO_2 diagram [28], of Dokhan volcanic flows show high-K (HK) suites; G- Plotting Dokhan volcanic samples in the Y+Nb vs. Rb diagrams of [29].

Using the geochemical total alkali versus silica (TAS) classification using diagram [27] shows that the present Dokhan volcanic lava flows are of andesite, dacite, rhyodacite, and rhyolite (Fig. 5D), while the basic dykes are of basaltic composition.Plot of the analysis samples in the SiO_2 versus K_2O+ Na_2O indicate that most lavas and the basic dykes are subalkaline(Fig. 5E). Applying the K_2O–SiO_2 diagram [28], the Dokhan volcanic flows are dominated by high-K (HK) suites and more high-K affinities in related to dacite to rhyolite lavas (Fig. 5F), the basic dykes show medium- to Low-K varieties. Plotting Dokhan volcanic samples in the Y+Nb vs. Rb diagrams [29],the andesite and dacite samples plottedin the Volcanic Arc Granites field into the area of post-collisional granites, while the rhyodacite and rhyolite samples ploted within the post-collision granite area at the boundary separating between Volcanic Arc Granites from Within Plate Granites (Fig. 5G).

3.2.2. Granites

Major element composition of the studied granite is shown in (Fig. 6A), SiO_2 ranges from 71.99 to 75.55, Al_2O_3 ranges from 12.16 to 13.89, Fe_2O_3, ranges from 1.46 to 2.18, K_2O ranges from 3.77 to4.7, Na_2O_3 ranges from 3.48 to 4.79, CaO ranges from 0.36 to 1.1, MgO ranges from 0.14 to 0.59, and TiO2 ranges from 0.19 to 0.41. Trace elements contents are shown in (Fig. 6B), it show an enrichments large ion lithophile elements (LILE), such as Ba, Sr, Rb, Pb and as well as the high field strength elements (HFSE) such as Zr and LREE, on the other hand it is depleted transition elements Ni, Co, Cr, and V and the other elements (HFSE) such as Nb and Th. The granite rocks are enriched in LREE such as La, Ce and Nd and are deplated in the other elements (Fig. 6C). On the total alkalis-silica (TAS) diagram [29] (Fig. 6D), the granite rocks fall in the granite field, whereas they are plotted on the alkali granite on the total alkalis versus silica (TAS) diagram (Fig. 6E) [30]. The plot of samples on the Na_2O+K_2O-CaO vs SiO_2diagram [31], ranges between alkalic toalkali- calcic rock series (Fig. 6F). Using the diagram of [32] to distinguishes between the different types of granites with SiO_2>68 wt.%,the present granite rocks plotted in the alkaline& highly fractionated calc-alkaline filed (Fig. 7A). The granitoids of the present study show both A/CNK values ≤1 and A/NK values >1 and applying the alumina saturation diagram [33], the granitic rocks of the study area are characterized by both metaluminous to peraluminous characteristics (Fig. 7B). In the FeO*/MgO versusSiO_2 diagram [34](Fig. 7C), the granitic rocks fall within the I&S -type fields. [35] used the Na_2O-K_2O binary diagram to discriminate between I-type, S-type and T-type granites and plots of the granite samples in this diagram it lie in the I-type granite field (Fig. 7D). Using the discrimination diagram for I and S-type granites [36] the studies granitic rocks plotted in the I-type granites (Fig. 7E).

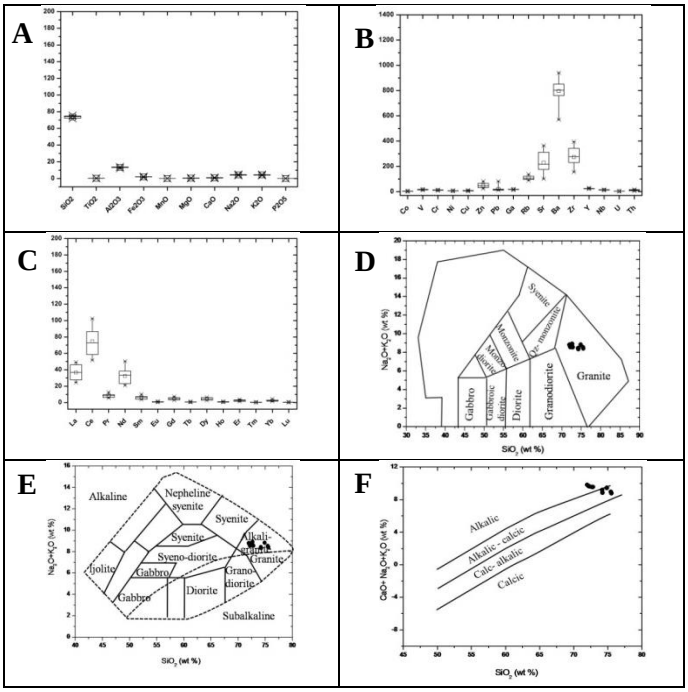

Figure 6: A, B and C- Box plot graphs showing the summary of geochemical data for granite rocks of major oxides (wt%) (A), trace elements (ppm) (B) and REE (ppm); D- Plots of granites in total alkala-silica (TAS) diagram of [30]; E- total alkalis versus silica (TAS) diagram after [27]of granites; F- Na_2O+K_2O-CaO vs SiO_2 diagram [31]of the granites range between alkalic to alkali- calcic rock series.

Applied tectonomagmatic discrimination Y + Nb vs. Rb and Nbvs Y diagrams **[29]**, all smaples plotted in the syn-collision granite and volcanic arc granite fields **(Fig. 7F and 7G)**. The chondrite normalized REE pattern of the granite sample is characterized by almost LREE-enrichment and , flat heavy REE patterns with moderately to strongly negative Eu anomalies **(Fig. 7H)**.

4. Discussion

4.1. Adakitic nature of the Dokhan Volcanic

Volcanic rocks in Wadi Hammad area are a part of Guruf Dokhan volcanics provenance that share a common intermediate to felsic rocks compositions with the Dokhan volcanic series in the Eastern Desert. **[37, 38]** used the geochemical data to distinguished between normal calc-alkaline lavas and these with adakitic characteristics, these data including Y (<18 ppm), Sr (>400 ppm), HREE (Yb< 1.9 ppm), Sr/Y(>40), and Al_2O_3 (>15 wt.%). On these bases, the present Dokhan lavas characterized by adakite nature **(Fig. 8A and B)**. This result is in agreement with many authors **[11, 39, 40]**. Eliwa etal. **[11]** indicate that adakitic lavas are common characteristics of the Dokhan volcanics in north Eastern Desert of Egypt and they are widely distributed in the area between Soahg-Safaga Highway (26º N) to the 27º50´N. However, A number of models for their formation have been suggested but debated extensively is still about their origin. Generally, two main models were suggested by the workers: (1) partial melting of an oceanic slab in an active subduction-related environment **[11]** and (2) adakite derived by partial melting of delaminated mafic lower crust interacting with overlying mantle-derived magma **[40, 25]**. Although the genetic connection between adakite and Cu-Au deposits confirmed in number of studies **[8, 2, 10, 41, 42]** argue are still about adakite mineralization **[43-45]**. The argument is that adakites, can be created in different ways: slab melting, melting of thickened crust, and fractional crystallization. Accordingly evolution of magma at the crustal levels (melting of thickened crust and fractional crystallization) is fundamental factor controls the Cu mineralization **[46, 47]**. Results of modelling by **[48]** show that adakites formed due slab melting (oceanic crust) have higher initial Cu and Au concentrations that could facilitate Cu-Au mineralization, but adakites formed due to partial melting of the lower continental crust and adakites formed due to fractional crystallization of mantle magma have low initial Cu and Au so that there are low chance for the ore to be formed. **[49]** stated that, the Cu concentration in oceanic crust is 2–4 times as high as the Cu abundances in the mantle and the continental crust. Therefore, according to **[49, 50]** slab melts are more favorable for spawning mineralization. Plotting the present data on the Sr/Y vs. $(La/Yb)_N$ **[51]**, K_2O/Na_2O vs. Al_2O_3 diagram **[52]**, and SiO_2 versus Mg# diagrams, indicate that the present Dokhan volcanic is adakitic in nature and formed due to slab melting **(Fg. 8C, D and E)**. Plotting the samples of Dokhan volcanics on La/Ce–Rb/Sr and Nb/U–Rb/Srdiagrams **[53] (Fig. 8F and G)**, show that they are similar to slab-derived adakites. Plotting of the samples on a Ni vs. Cr diagram **[54]** shows that the present adakitic rocks plotted along and around the mixing line between primitive mantle and slab melt **(Fig. 8H)** and accordingly, these rocks are favorable site for the formation of Cu-Au deposits.

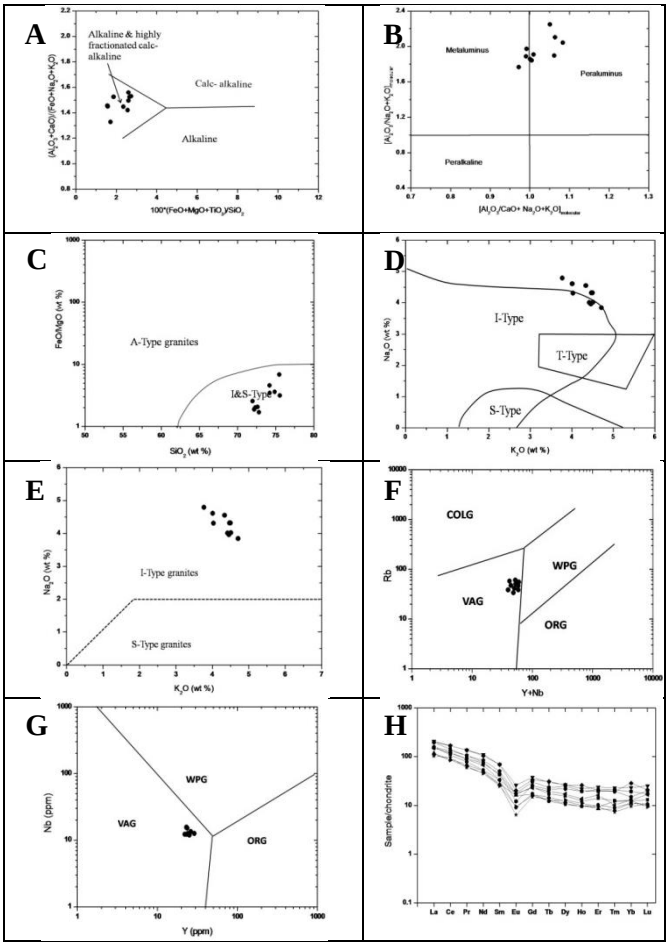

Figure 7: A-plotting granite samples onSylvester [32]diagram; B-Plotting granite samples of A/CNK vs. A/NK diagram after Shand[33]; C- Plotting granite samples onFeO*/MgO versus SiO2 diagram [34]; D- Plotting granite samples on Na2O-K2O binary diagram[35]; E- Plotting granite samples on Na2O-K2O binary diagram [36]; F and G Plotting granite samples on tectonomagmatic discrimination Y + Nb vs. Rb and Nbvs Y diagrams [29]; H-Chondrite normalized REE pattern of the granite samples.

4.2. Physico-chemical characteristics of granitic magma

Geochemically, water and other volatile or fluxing elements are important factors controlling oxygen fugacity in igneous processes **[55, 56]**. Major and trace element contents and variation trends of Hammad granite are used in the prediction of their oxidation state. Also examine the genetic link between the oxidation state of granites and the processes leading to Cu–(Au) mineralization. Plotting the granitic intrusive rocks from the Hammad area on the schematic plot of

degree of fractionation (Rb/Sr ratio) versus the oxidation state (Fe_2O_3/FeO) **[57]** which is used for predicting magmatic-hydrothermal mineralisation related to the I-type granitoids; show a marginal metaluminous to peraluminous and moderalty oxidized, the plotted sample occupy the field of Cu-Au with marginal amount of W and W-Mo fields **(Fig. 9A)**. The Fe_2O_3/FeO ratios for granite samples are range between 0.87 and 0.92 with an average 0.88, and samples plotted close to the boundary between magnetite- and ilmenite-series granitoids on a SiO_2 versus Fe_2O_3/FeO diagram **[58]** and the majority of the granite samples occur in the Porphyry Cu –granitoids field after **(Fig. 9B)**. Using A/NK vs A/CNK diagram **[59, 60]** Hammad granites pluton representbyI-type (A/CNK ratio<1.1) and show predominantly metaluminous to weakly peraluminousc haracteristic **[36]**. In addition, based on these presented results, the Hammad granite has high metallic ore potential, where all samples occur in the Cu-Au, Au (Bi) mineralization field with small overlap with W mineralization type **(Fig. 9C)**.

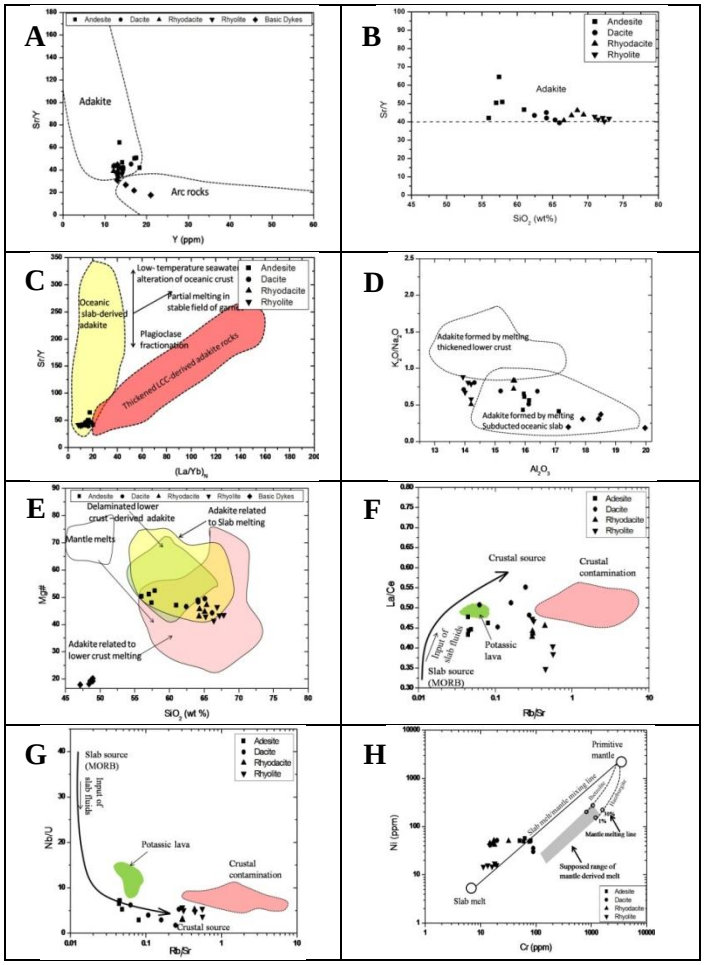

Figure 8: A- Y vs. Sr/Y diagram **[37]** show adakitic nature of Dokhan volcanics; B- Plotting Dokhan volcanics samples on Sr/Y vs. SiO_2 diagram; C- Sr/Y vs. La/Yb correlation diagrams **[51][48]**; D-K_2O/Na_2O vs. Al_2O_3 diagram of Dokhan adakites **[52]**; E- $Mg_{\#}$ vs. SiO_2, fields indicating adakites related to slab melting. F- Plotting Dokhan volcanics samples on La/Ce vs. Rb/Srdiagram after Hou et al. (2004); G- Plotting Dokhan volcanics samples onNb/U–Rb/Srdiagram **[53]**. H- Plotting of Dokhan samples on a Ni vs. Cr diagram **[54]**.

Oxidized magmas have a greater capacity to dissolve sulfur and metals and transport them to shallow crustal levels were the high-water content is required to form a hydrothermal system. Ballard et al.**[61]** suggested that oxidation conditions of magma may be used in the exploration for intrusions hosting porphyry-type mineralization. High magmatic oxidation states are also, favorable for the formation of major Au-(Cu) mineralization. Oxidation states of the Wadi Hammad granitoids play essential role in the formation of the mineralization, where the granite rocks have relatively restricted range of oxidation state, Using ΔOx vs. FeO_t diagram **[62]**, where ΔOx $\log_{10}$ = (Fe_2O_3/FeO) +0.3+ 0.03×FeO*, where FeO* = total Fe expressed as FeO **[62]**, all samples aretransitional between moderately and strongly oxidised granites **(Fig. 9D)**. According to **[62]**, these granites should be prospective for Au-Ag associations in both vein and epithermal. Plotting samples on the FeO +MnO-Fe_2O_3 + TiO_2-MgO ternary diagram **[63, 64]** the Hammad granite rocks are oxidized as characterized by high Fe^{3+}/Fe^{2+} ratios **(Fig. 9E)**. The oxidation states of the granite rocks can also predicated using AFM diagram **[65]** that separated between the tholeitic and calcalkaline characteristic nature, the Hammad samples show a calc-alkaline character, this trend is indicative for a felsic magma type that show a high oxygen fugacity in the parent melts which lead to the crystallization of magnetite with SiO_2 increase, resulting in the calcalkalinetrends **[55, 66, 67] (Fig. 9F)**. Since evolution of parental magmas at shallow crustal levels is an essential step in the process conducive to porphyry-Cu and related deposits. The Rb-Sr variation diagram **[68]** shows that the investigated granites was situated at crustal thickness ranging from 20 to 30 km **(Fig. 9G)** (relatively shallow tomoderate depths **[69]**, according to the presented data here the Rb/Sr ratio of the studied granite proved useful information of magmatic differentiation, as Rb/Sr ratio increases with higher degree of differentiation. The Rb/Sr vs. SiO_2binary diagram **(Fig. 9 H)** indicates that these granites have been derived from highly differentiated and more evolved granitic liquids. Determination of temperature of the intrusive rocks is important for definition of petrogenesis, regional tectonism and the associated ore deposits. Whole-rock are used to obtain temperatures of Hammad intrusive rocks,TiO_2vs SiO_2 **[70]** contents indicate values well below 900 °C **(Fig. 9 I)** and P_2O_5vs SiO_2 **[71]** give values around 800°C **(Fig. 9J)**. These temperature values are related to titanite and apatite minerals, suggest that the Hammad granites magmastarted to crystallize attemperatures of800°C and refer toHigh temperature I-typegranites. Sum of the above discussion can come to the conclusion; Hammad granite intrusive rocks are characterized by: 1. predominantly metaluminous to weakly peraluminous, 2. span the boundary between the ilmenite-magnetite series, 3. transitional between moderately and strongly oxidized granites, 4. Situated at relatively shallow to moderate depths (20 to 30 km), 5. Hammad granites magma started to crystallize at temperatures around 800 °C, 6. characterized by sub-alkalic nature, 7. associated with the quartz-bearing mineralization and 8. High evolved and fractionated granite. Accordingly, the intrusive rocks inWadi Hammad area and the associated mineralization met the main characteristics of Intrusion-Related Gold Deposits (IRGD) **[7, 72, 73]**.

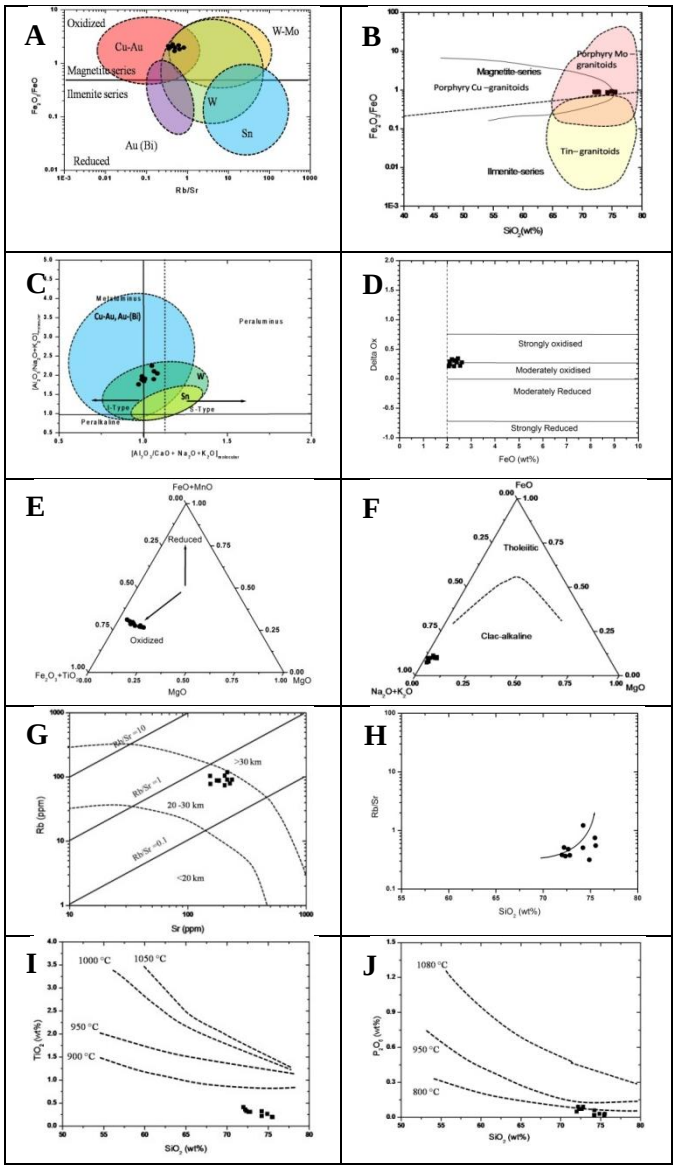

Figure 9: A- Plotting the granitic rocks on Rb/Sr versus Fe_2O_3/FeO diagram **[57]**. B- SiO_2 versus Fe_2O_3/FeO diagram **[58]**; C- Plotting granite samples on A/NK vs A/CNK diagram **[59-60]**; D- Using ΔOx vs. FeO_t diagram **[62]**; E- Plotting granite samples on the FeO + MnO-Fe2O3 + TiO2-MgO ternary diagram modified **[63][64]**; F- AFM diagram of granite rocks **[65]**; G- The Rb-Sr variation diagram **[68]** show depths of emplacement of the intrusive granite; H- Plotting granite smaples on Rb/Sr vs. SiO_2 binary diagram; I- TiO_2vs SiO_2 diagram **[70]** show crystallize at temperatures of granite rocks; J- Estimating granite crystallize temperatures using P_2O_5vs SiO_2 diagram **[71]**.

4.3. Metallogenic implications

There is a general consensus that ore fluids precipitating lode gold deposits in Precambrian cratons are of metamorphic origin, liberated during greenschist to amphibolite facies metamorphism **[74, 75]**. The rarity or absence of metamorphosed supracrustal rocks in the North Eastern desert in general and in the study area in particular **[76, 77]** rules out the metamorphic derivation for the ore fluids responsible for gold mineralization.Notably, the occurrences of Dokhan volcanics with adakitic nature **[11]**, and the close temporal–spatial relationship with the Au mineralization **[78, 79]**, inspirited the authors to estimate that the source of gold mineralizations in Hammad area are related to these adakitic Dokhan volcanics. Although the genetic connection between adakite and Cu-Au deposits confirmed innumber of studies **[2] [8, 10, 41, 42]**, argue are still about adakite mineralization **[43-45]**.

The argument is that adakites can be created in different ways: slab melting, melting of thickened crust, and fractional crystallization. Accordingly evolution of magma at the crustal levels (melting of thickened crust and fractional crystallization) is fundamental factor controls the Cu mineralization **[46, 47]**. Results of modelling by **[48]**, show that adakites formed due to slab melting (oceanic crust) have higher initial metal concentrations that could facilitate mineralization, whereas adakites formed due to partial melting of the lower continental crust and adakites formed due to fractional crystallization of mantle magma have low initial metal, so that there are low chance for the ore to be formed. Sunet al. **[49]** stated that the metal concentration in oceanic crust is 2–4 times as high as the metal abundances in the mantle and the continental crust. Therefore, according to Ling el al. **[49, 50]** slab melts are more favorable for formation of mineralization.

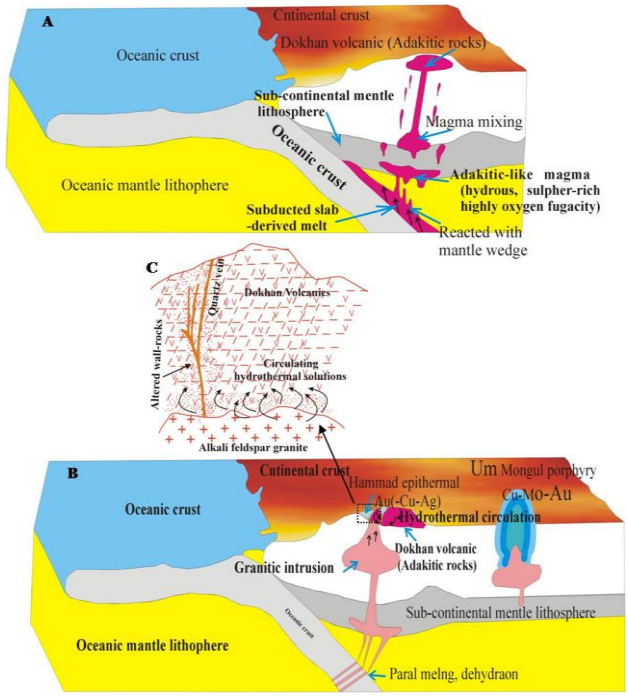

Figure **10**: Genetic model for Au (Cu)-mineralization at Hammad area: A) Schematic illustration showing formation adakitic volcanic rocks in subduction zones due slab melts; B) Schematic illustration showing formationGabal Al-Guluf granite intrusion due to magma fractionation caused an enrichment of water and volatiles; C) The intrusion of the high oxidizing, water- and volatile-rich alkaline and alkalie-calcic magma into the adakiticDokhan volcanic leads to circulation of these fluids in the latter leaching the available metals (Au and base metals), the leached metals are deposited in preexisting open fissures at the cold end of convective cells near the surface form Au (Cu)-rich quartz veins.

Field observations show that Au-Cu ore bodies in Hammad area represented mainly by structurally controlled mineralized quartz vein and the surrounding alteration and are located generally at the contact or within Dokhan volcanic and granitic intrusion. In addition, using the geochemical discrimination diagrams, indicate that the adakitic Dokhan volcanic formed by slab-melting and it is favorable site for the formation of Cu (Au) deposits **(Fig. 10A)**. The genetic relationship between ore-related intrusions (IRGD) and Au mineralization is a key problem in constraining the origin of the gold deposits and in formulating their prospecting criteria **[80]**. Detailed geochemical and mineralogical studies reveal that Hammad deposits are spatially closely related and associated with granitic intrusion. Detailed geochemical and mineralogical studies reveal that Hammad granitic intrusion belong to Intrusion-Related Gold Deposits (IRGD) and are characterized by alkaline, magnetite-series, I-type granites affinity and high-K. Notably, they have high Ba/Sr (average 4) and K/Rb (average 340) ratios, and low Rb/Sr ratios (0.5), which are much productive of Au mineralization **[81]**. The estimated temperatures of the granite samples of about 800°C show a high temperatures, implying volatile rich compositions of the magmas **[81, 82]**. The existence of amphibole and biotite, and associated accessory minerals particularly magnetite and sphene indicate their formation under high oxidizing conditions **[81, 83]**, these mineralogical results supported by the geochemical study **(Fig. 10B)**. Oxidized magmas have a greater capacity to dissolve sulfur and metals and transport them to shallow crustal levels were the high-water content is required to form a hydrothermal system **[61]**. Accordingly, the high oxidizing, water- and volatile-rich magma, and alkaline to alkali-calcic compositions of the studied Gabal Al-Guluf granites in Hammad area, in addition to its high temperature of formation are favorable for leaching Au and Cu from the adakitic Dokha nvolcanics, transferring them into fluid phase **[61, 81] (Fig. 10C)**. High temperature granites are more favorable for mineralization formation, not only due to their higher temperature but also due to their high capacity of fractional crystallization leading to concentration of incompatible elements, with progressive increase in the activity of H_2O **[83-86]** suggested that the granitic intrusion served as a heat engine that drove circulating hydrothermal fluids through the fractures. The formation of Hammad deposits can be interpreted as follows:1) Magma fractionation caused an enrichment of water and volatiles, represented by Gabal Al-Guluf granite intrusion, 2) The intrusion of the high oxidizing, water- and volatile-rich magma, and alkaline to alkalie-calcic into the adakitic Dokhan volcanic leads to circulation of these fluids in the latter leaching the available metals (Au and base metals), 3) The leached metals are deposited in preexisting open fissures at the cold end of convective cells near the surface form Au (Cu)-rich quartz veins **(Fig. 10B)**.

4. Conclusion

Geological, mineraological and geochemical studies on Wadi Hammad mineralization revealed that:

[1] Wadi Hammad mineralization is polymetallic vein-type and represented by mineralized main quartz vein, silicified shear zone, associated hydrothermal alterations and breccia zone.

[2] The mineralization occurs in the contact between Dokhan volcanics and Younger granites and confined to and controlled by Wadi Hammad shear zone.

[3] Dokhan volcanics have adakitic nature and formed by slab melt and are favorable for Cu-Au mineralization.

[4] The intrusive granite rocks are characterized by metaluminous to weakly peraluminous, span the boundary between the ilmenite-magnetite series, transitional between moderately and strongly oxidized granites, situated at relatively shallow to moderate depths (20 to 30 km), and started to crystallize at temperatures around 800 °C.

[5] Shearzone and fault system channelled upand transported substantial quantities of heat and strongly oxidizing, water- and volatile-rich magma to the early formed adakitic rocks leaching the available metals such as Au and base metals.

[6] The leached metals are deposited in preexisting open fissures forming Au (Cu)-rich quartz veins.

References

[1] A. R. Drysdall, C. J. Douch, *Journal of African. Earth Science*, 4 (1986)275-288.

[2] S.M. Kay, Mpodozis C., Coira B., *Society of Economic Geologists, Special Publication*, 7 (1999)27–59

[3] R. H. Sillitoe, *Reviews in Economic, Geology*, 13(2000)315–344.

[4] R. M. Tosdal, J. P. Richards, *Reviews in Economic, Geology* ., 14 (2001)157–181

[5] A. A. Surour, *The Geology of the Egyptian Nubian Shield. Regional Geology Reviews. Springer, Cham.*, (2021).

6] Y. El-AbdRahman, T. Seifert, A. Said, *Ore Geology Reviews.*, 99 (2018)217-234

[7] N. S. Botros, *Acta Geologica Sinica (English Edition)*, 95(3)(2021)1033–1055

[8] D. Thie´ blemont, G. Stein J. L. Lescuyer, Gisements e´,. *Comptes rendus de l'Académie des Sciences Paris*, 325 (1997)103–109

[9] F. G. Sajona, R. Maury, *Comptes rendus de l'Académie des Sciences Paris*, 326 (1998)27–34

[10] R. Oyarzun, A. Ma´ J. rquez, Lillo, I. Lo´ pez, S. Rivera, *Mineral Deposita*, 36 (2001)794–798.

[11] H.A. Eliwa, , J. I. T. KimuraItaya, *Precambrian Research*, 151 (2006)31–52.

[12] J.W. Hedenquist, J.B. Lowenstern, *Nature*, 370(1994)519-527

[13] D. J. Blundell, *Geological Society, London, Special Publication*, 204 (2002)1–12.

[14] C. G. MacPherson, R. Hall, *Geological Society, London, Special Publications*, 204 (2002)49–68

[15] M.E. Barley, P. Rak, D.Wyman, *Geological Socety of London Special Publications*, 204 (2002)39-47

[16] L.D. Setijadji, S. Kajino, A. Imai, K. Watanabe, *Resource Geology*, 56 (2006)267-292

[17] M. Chiaradia, *Nature Geoscience*, 7 (1) (2014)43-46.

[18] K. I. Khalil, M. El-Roz, M. H. Shalaby, Arslan, A. I., *International Confrance on geochemistry, Alex. Univ., Egypt.*, I (2006)169-190.

[19] A. Osman, *Mineral deposits: possessing. Balkema, Rotterdam*, (1999) 189-192.
[20] A. Osman, H. Kucha, A. Piestrzynski, *Mineralogy and Petrology*, 31(2) (2000)17-30
[21] B. B. Nasr, M. S. Masoud, H. El Sherbeni, A. A. Makhlouf, *Annals Geological. Surve of Egypt*, V.XXI (1998)331-344.
[22] F.F. Basta, A.E. Maurice, B.R. Betros, M. K. Azer, A. El-Sobky, *Lithos*, 288 (2017)248–263.
[23] H.A. Khamis, *Master of Science. Thesis, Cairo Univ., Egypt*, (1995) 235 p.
[24] E. A. Khalaf, *Bulletin of Volcanology*, 75 (2013)1-31
[25] , B. A. Abuamarah M. K. Azer, P. D. Asimow, Q. Shi, *Lithos*, 388 (2021) 389: 106051
[26] H. El Sundoly, I. Azab, H. Khamis, *Annals Geological. Surve of Egypt*, XXXVIII (2021)97 - 111.
[27] K.G. Cox, J.D. Bell, R.J. Pankhurst, *The Interpretation of Igneous Rocks. Allen &Unwin, London*, 1979.
[28] R. W. Le Maitre, P. Bateman, A. Dudek, J. Keller, J. Lameyre, M. J. Le Bas, P. A. Sabine, R. Schmid, H. Sorensen, A. Streckeisen, A. R. Woolley, B. Zanettin, *A classification of igneous rocks and glossary of terms: recommendations of the International Union of Geological Sciences subcommission on the systematics of igneous rocks. Blackwell* ,Oxford 1989.
[29] J. Pearce, N. Harris, A. Tindle, *Journal of Petrology*, 25 (4) (1984)956–983
[30] E. A. K. Middlemost, *Earth-Science Reviews, 31*(1991)73-87
[31] B. R. Frost, C. G. Barnes, W. J. Collins, R. J. Arculus, D. J. Ellis, C. D. Frost, *Journal of. Petrology*, 42 (2001)2033–2048.
[32] P. J. Sylvester, *Journal of. Petrology*, 97 (1989)261–280.
[33] S. J. Shand, *The Eruptive Rocks , 2nd edn. New York: John Wiley*, (1943)444 pp.
[34] B. W. Chappell, A. J. R. White, *Pacific Geology*, 8(1974)173–174.
[35] T. Liew, F. Finger, V. Hock, *Chemical Geology*, 76 (1989)41-55.
[36] B.W. Chappell, A.J.R. White, *Beijing Science Press*, (1984)87–101
[37] M. J. Defant, M. S. Drummond, *Nature*., 347 (1990) 662–665
[38] M. J. Defant, M. Drummond, S. Mount, T. HelensS. *Geology*, 21 (1993)547–550
[39] K.M. Abdelfadil, M. A. Obeid, M. K. Azer, P.D. Asimow, *Journal Asian Earth Science*, 158 (2018)301–323.
[40] M. A. Obeid, M. K. Azer, *Intinational Journal Earth Science*, 104 (2015)541–563
[41] R. Oyarzun, A. Marquez, J. Lillo, I. Lopez, S. Rivera, *Mineralium Deposita*, 37 (2002)795–799.
[42] R.W. Kay and S. M. Kay, *Acta Petrologica Sinica*, 18 (2002)303–311.
[43] O. M. Rabbia, L. B. Hernandez, R.W. King, L. Lopez-Escobar, *Mineralium Deposita*, 37 (2002) 791–794.
[44] J.P. Richards, *Mineralium Deposita*, 37 (2002)788–790.
[45] J.P. Richards, R. Kerrich, *Economic Geology*, 102 (2007)537–576.
[46] T. Bissig, A.H. Clark, J.K.W. Lee, A. von Quadt, *Mineralium Deposita*, 38(2003)844–862.
[47] P. Hollings, D. Cooke, A. Clark, *Economic Geology*, 100 (2005) 887–904
[48] W.D. Sun, H. Zhang, M. Ling, X ,Ding, S. Chung, J. Zhou, X. Yang, W. Fan, *International Geological. Review, 53* (2011) 691–703
[49] W. D. Sun, M. X. Ling, X. Y. Yang, W. M. Fan, X. Ding, H.Y. Liang, *Science China – Earth Sciences*, 53 (2010) 475–484.
[50] M. X. Ling, F. Y. Wang, X. Ding, Y. H. Hu, J. B. Zhou, R. E. Zartman, X. Y. Yang, W. D. Sun, *Economic Geology*, 104 (2009) 303–321
[51] Y. S. Liu, S. Gao, Z. C. Hu, C. G. Gao, K. Q. Zong, D. B. Wang, *Journal of Petrology*, 51 (2010) 537–571
[52] J. H. Liu, C. M. Xie, C. Li, M. Wang, H. Wu, X. K. Li, Y. M. Liu, T. Y. Zhang, *Lithos*, 296–299 (2018) 265–280
[53] Z. Q. Hou, Y. F. Gao, X. M., Qu, Z. Y. Rui, X. X. Mo, *Earth and Planetary Science Letters*, 220 (2004) 139–155.
[54] N. Tsuchiya, S. Suzuki, J. I. Kimura, H. Kagami, *Lithos*, 79 (1) (2005) 179-206.
[55] E. F. Osborn, *American Journal of Science*, 257(9) (1959) 609-647.
[56] G. K. Czamanske, D. R. Wones, *Journal of Petrology*, 14 (1973) 349 –380.
[57] P. L. Blevin, B. W. Chappell, C. M. Allen, *Earth Sciences*, 87 (1996) 281–290.
[58] R. D. Taylor, J. M. Hammarstrom, N. M. Piatak, R. R.. Seal, *Geological Survey Scientific Investigations Report*, 5070–D 2012 (2010) p.64.
[59] P. D. Maniar, P. M. Piccoli, *Geological Society of America Bulletin*, 101 (1989) 635-643.
[60] L. D. Meinert *Mineralogical Association of Canada Short Course Series*, 23 (1995) 401-418
[61]Ballard, J.R., Palin, M. J., Campbell, I. H., *Contributions to Mineralogy and Petrology* , 144 (2002)347–364
[62] P. L. Blevin, *Resource Geology*, 54 (3) (2004) 241–252.
[63] B. W. Chappell, A. J. R. White, *Earth Sciences*, 83(1992) 1-26.
[64] F. Rabayrol, C. J. R. Hart, *Mineralium Deposita*, 56 (2021) 279–306.
[65] H. Kuno, Differentiation of basalt magmas. In: H.H. Hess and A. *Interscience, New York, N.Y.*, 2 (1968) 623-688.
[66] P. Vermeesch, V. Pease, *Geochemical Perspectives Letters*, 19 (2021) 1–6.
[67] H. Mollai, S. Hashemi, M. Kardani, *Yeues Jahrbuch für Geologie und Paläontologie*, 273 (3) (2014) 277–297
[68] K. C. Condie, *Geological Society of America Bulletin*, 84 (1973) 2981-2991.
[69] K. Fawzy, *Open Journal of Geology*, 7 (2017) 93-117.
[70] M. Kwékam, V. Talla, E. M. Fozing, k. Tcheumena J. Kouémo, I. Dunkl, E. Njonfang, *Frontiers in* Earth Science, 8 (2020) 363.
[71] T. H. Green, E. B. Watson, *Contributions to Mineralogy and Petrology*, 79 (1982) 96–105
[72] R. H. Sillitoe, *Gold metallogeny and exploration. Springer, Boston, MA.*, (1991) 165–209.
[73] J. F. H. Thompson, R. H. Sillitoe, T. Baker, J. R. Lang J. K. Mortensen, *Mineralium Deposita*, 34 (1999) 323-334.
[74] D. I. Groves, M. Santosh, J. Deng, Q. Wang, L. Yang L.

Zhang, *Mineralium Deposita*, 55 (2020) 275–292.
[75] D. A. Wyman, K. F. Cassidy, P. Hollings, *Ore* Geology *Review,s* 78 (2016) 322-335
[76] S. El-Gaby, F. K. List, R.. Tehrani, *The pan-African belt of Northeast Africa and adjacent areas. Vieweg&Sohn, Weisbaden,* (1988) 17–68.
[77] R. J. Stern *Journal of African Earth Sciences*, 146 (2018) 15-27.
[78] T. G. Ivanov, A. A. Hussein, *Egyptian Geological Survey, Internal report*, (1972) 68/73
[79] N.S. Botros, *Annals of the Geological Survey of Egypt*, 20 (1995) 381 – 409.
[80] C. C. Han, X.B. Zhang, S. S. Wu, Y. T. Liu, *Minerals*, 12 (2022) 485.
[81] L. Li, M. Santosh, S. R. Li, *Ore Geology Reviews*, 65 (2015) 589-611.
[82] G. Y. Chen D. S. Sun X. R. Zhou W. Shao, R. T. Gong Y. Shao *China University of Geosciences Press*, (1993) 1-230
[83] N. Li, Y. J. Chen, X. H. Deng, J. M. Yao, *Ore* Geology *Review,s*, 63 (2014) 520–531.
[83] B. W. Chappell, C. J. Bryant, D. Wyborn, A. J. R. White, I. S. Williams, *Resource Geology*, 48 (1998) 225–235.
[84] M. Kwékam, I. Dunkl, E. M. Fozing, G. Hartmann, T. Njanko, J. TcheumenakKouémo, *Geological Society*, 502 (2020) 19.
[85] M. A. Takla, A. A. El Dougdoug, M. A. Gad, A. H. Rasmay, H. K. El Tabbal, *Annals of the Geological Survey of Egypt*, 5 (199) 20: 411 – 432.
[86] M. A. Takla, A. A. El Dougdoug, A. H. Rasmay, A. A. Gad, H. K. El Tabbal, *Egyptian. Mineralogist*, 2 (1990) 3 – 20.